J Appl Physiol 99: 2369–2378, 2005.
First published August 18, 2005; doi:10.1152/japplphysiol.00486.2005.

In vitro time-dependent response of periodontal ligament to mechanical loading

Colin S. Sanctuary,[1] H. W. Anselm Wiskott,[2] Jörn Justiz,[1] John Botsis,[1] and Urs C. Belser[2]

[1]*Laboratory of Applied Mechanics and Reliability Analysis, Swiss Federal Institute of Technology, Lausanne; and* [2]*School of Dental Medicine, University of Geneva, Geneva, Switzerland*

Submitted 27 April 2005; accepted in final form 18 July 2005

Sanctuary, Colin S., H. W. Anselm Wiskott, Jörn Justiz, John Botsis, and Urs C. Belser. In vitro time-dependent response of periodontal ligament to mechanical loading. *J Appl Physiol* 99: 2369–2378, 2005. First published August 18, 2005; doi:10.1152/japplphysiol.00486.2005.—This study examined the time-dependent response of bovine periodontal ligament (PDL). Applying linear viscoelastic theory, the objective was *1*) to examine the linearity of the PDL's response in terms of its scaling and superposition property and *2*) to generate the phase lag-vs.-frequency spectrum graph. PDL specimens were tested under three separate straining conditions: *1*) tension ramp tests conducted at different strain rates, *2*) pulling step-straining to 0.3 in discrete tests and to 0.3 and 0.6 in one continuous run, and *3*) tension-compression sinusoidal oscillations. To this effect, bar-shaped specimens of bovine roots that comprised portions of dentin, PDL tissue, and alveolar bone were produced and strained in a microtensile machine. The experimental data demonstrated that neither the scaling nor the superposition properties were verified and that the viscoelastic response of the PDL was nonlinear. The PDL's elastic response was essentially stiffening, and its viscous component was pseudoplastic. The tangent of the PDL's strain-stress phase lag was in the 0–0.1 range in the tensile direction and in the 0.35–0.45 range in the compressive direction. In line with other biological tissues, the phase lag was largely independent of frequency. By use of the data generated, a mathematical model is outlined that reproduces both the elastic stiffening and viscous thinning of the PDL's response.

elasticity; viscosity; nonlinearity; mechanical stress

THE MECHANICAL LINK BETWEEN a tooth and the surrounding bone is provided by the periodontal ligament (PDL). Within this tissue, three systems control the dynamics of the tooth under load: *1*) the fibrous component (collagen and elastic fibers), *2*) the ground substance, and *3*) the vasculature. Specific functions are ascribed to each system. The collagen fibers are regarded as active in tension. In compression, it is the glycans of the ground substance that assume the damping. In effect the glycans form a biphasic medium with water. During loading, their spatial arrangement is altered as a function of their water-binding capacity, which in turn conditions their macromechanical properties (swelling, viscosity, and resistance to flow under shear loading) (26). With respect to the vasculature, it is reasoned that arterial blood pressure has a stabilizing effect on the root (45).

Whether the functions of the three systems can actually be separated as described above is debatable because all three are highly interrelated. Furthermore, the anatomic contingencies of the PDL are such as to reciprocate some movements; i.e., tension on one side of the alveolus may imply compression on the other. Indeed, besides vertical loads, teeth are also subjected to horizontally directed force vectors (13). Hence the PDL is not active in tension only (as in tendons, muscles, or articular ligaments) but in compression as well. To provide a global view of the PDL's response to mechanical loads, a host of numerical analyses was proposed (20, 30, 33, 37, 42). These analyses are based on sets of equation systems (i.e., the constitutive laws) that model the response of PDL tissue. The constitutive laws establish the relationship between the applied strains and the resulting internal stresses (7) whereby nonlinearity of the elastic or the viscous component of the PDL substantially increases the complexity of the equation systems.

Ideally such equation sets should be "robust"; that is, the equation that models the tissue's behavior is controlled by parameters that reflect true material properties (and should not be written as any "best fit" function). In effect, the coefficients of most best fit functions are empirical, have no physical interpretation, and vary with the experimental conditions. By contrast, a constitutive law is derived from physical principles, and often its coefficients are material parameters. To determine these parameters, plain specimens of well-defined geometries that are subjected to elementary load conditions are required. One such test is the tension test, which has been applied by a number of authors (2, 10). From such tests, material parameters such as modulus, strength, uniaxial maximizer strain, and strain energy density can be determined (31). However, accurate numerical modeling of PDL behavior requires additional data. Indeed, available clinical and experimental evidence indicates that the response of the periodontal ligament is both elastic and viscous (9, 42), whereby it is commonly accepted that the elastic component is nonlinear (3, 41, 46, 49). Whether the PDL's viscosity is or is not linear has not been established. In this regard, load-displacement experiments conducted as ramps, relaxation tests, and sinusoidal stimuli will assist in determining the time-dependent response of the tissue sample. Time dependency, which is often conceptualized as a dashpot, characterizes the essence of viscosity (in contrast to elasticity in which all deformations are instantaneous).

To optimize the constitutive laws presently being developed in our laboratory, the objective of the present study was to further characterize the time-dependent behavior of the PDL under monotonic ramp tests and sinusoidal strains under various frequencies. Such constitutive equations are instrumental in predicting the stresses and strains that develop in the oral cavity. They link the forces generated by the masticatory musculature to tooth displacements, local stress concentrations, and possible hard tissue failure.

MATERIALS AND METHODS

Overview

Specimens of PDL tissue were subjected to specific load profiles to characterize the PDL's response *1*) by examining its linearity of

Address for reprint requests and other correspondence: H. W. A. Wiskott, School of Dental Medicine, Univ. of Geneva, 19, rue Barthélemy-Menn, 1205 Geneva, Switzerland (e-mail: anselm@wiskott.com).

The costs of publication of this article were defrayed in part by the payment of page charges. The article must therefore be hereby marked "*advertisement*" in accordance with 18 U.S.C. Section 1734 solely to indicate this fact.

response, *2*) by evaluating the relationship between the elastic and the viscous component in terms of the phase lag between applied strain and resulting stress, and *3*) by further characterizing the time-dependent response using strain ramps to rupture. To obtain specimens in large numbers, bovine teeth were used for testing. Bar-shaped specimens comprising portions of dentin, PDL, and bone were produced and subjected to monotonic ramps and oscillatory tests in a microtensile machine.

In a first series, the scaling property was examined by conducting ramp tests at different strain rates. The resulting load-response curves were then divided by the strain rate to determine whether they could be reduced to one single elementary curve (in colloquial terms: whether they would "collapse"). If such collapsing was observed, the first condition for linearity (i.e., scaling) was satisfied. Then the ramp data were replotted to more specifically identify the effect of the viscous component on the overall response. In a second series, the superposition property was examined by subjecting the specimens to step-strain-relaxation tests at two levels. The objective of this procedure was to determine whether the response of a single two-step run could be duplicated by adding the values obtained on two separate single-step tests. If such a superposition was observed, the second criterion for linearity (i.e., superposition) was fulfilled. In a third series, sinusoidal strains at various frequencies were applied to the specimens. Alterations in the shape of the stress response, the phase lag between the applied strain, and the recorded stress as well as the phase lag-vs.-frequency relationship were recorded. Last, the specimens were pulled to rupture at three different rates to augment the data on the time-dependent properties as well as to further characterize the material parameters of the PDL tissue.

Data Analysis

Linearity of response. For a tissue to present linearity of response to external straining, two conditions must be met: scaling (homogeneity) and superposition (additivity).

The scaling property holds when $S[\alpha \cdot E(t)] = \alpha \cdot S[E(t)]$ with S = stress, E = strain, α = scalar, and t = time. In the present study the scaling property was examined by use of ramp tests. Taking α as the strain rate, the data were replotted as $\hat{S} = S(t)/\alpha$ vs. $\hat{E} = E(t)/\alpha$. The scaling property is verified when the plot $\hat{S}$ vs. $\hat{E}$ is independent of the strain rate. Graphically, this translates into a set of curves that all collapse into a single line.

For a tissue to present the superposition property, the following relation must apply: $S[E_1(t) + E_2(t)] = S[E_1(t)] + S[E_2(t)]$, which implies that the input strain histories do not interact (47). In the present work, superposition was verified by using step-strain relaxation tests. In the presence of a linear response all experimental stress-relaxation curves may be superimposed by addition or subtraction, hence the usual denomination of "superposition of separate responses."

It must be noted that the existing analytical tools (i.e., verification of the scaling and superposition properties) are solely meant to determine whether a viscoelastic system is linear or not. Should this not be the case, they are not capable of distinguishing whether it is the elastic, the viscous, or both components that are responsible for the nonlinearity observed. Although the elastic component of soft tissues, including the PDL, is essentially nonlinear, the behavior of the viscous (i.e., fluid) component has not been assessed. A sensible approach for differentiating between both components is to use available analytical tools and to conduct appropriate tests so that they maximize the effect of either the elastic or the viscous component. To this end, our reasoning was as follows.

The mechanical analog to linear viscoelastic material systems may be visualized as combinations of springs (i.e., the elastic component) and dashpots (i.e., the viscous component). Hence the total stress response (S) may be expressed as a function $S = F(E,\dot{E},\kappa,\eta)$ with E as strain, $\dot{E}$ as the strain rate, κ characterizing the stiffness of the spring, and η the viscosity. In a broad view of such a system, κE expresses the elastic component of the response and $\eta\dot{E}$ the viscous contribution. Assuming that at the early stages of deformation the PDL fibers uncoil without supporting significant load and that the fluid component dominates the deformation behavior, then the $\eta\dot{E}$ component is the primary contributor to the stress response. Therefore, as a first-order approximation, S is reduced to $S \approx \eta\dot{E}$. To test the linearity of the viscous component, the experimental data obtained from constant rate monotonic loading were thus rearranged to produce a plot depicting S as a function of $\dot{E}$ at different levels of $\dot{E}$. If the viscous component is linear, the relationship expresses itself as a straight line from the origin. If not, it means that η varies with the strain rate, which in turn implies that the viscous component is not linear.

Phase lag. To understand the deformational mechanisms occurring within a tissue, one technique consists in subjecting the samples to harmonic oscillatory strains. Relative to the applied stimulus, the response may then be decomposed into an "in-phase" and an "out-of-phase" component. In a linearly viscoelastic system, the in-phase component represents the elastic response and indicates the tissue's ability to store energy, whereas the out-of-phase component represents the viscous response and is proportional to the energy that is irrecoverably dissipated.

The difference between the peak applied strain and the peak resulting stress is called phase lag and is expressed as an angle (δ). The tangent of δ is proportional to the ratio between the energy that is dissipated and the energy that is stored in the system. For perfectly elastic materials, δ equals 0. For Newtonian liquids, δ is 90° ($\pi/2$), and for viscoelastic systems, $0 < \delta < 90°$. Tan δ is also referred to as "loss tangent" or "damping factor" and is regarded as a key parameter in understanding the transitions between different deformational mechanisms.

In the present study, the phase lags were determined and plotted against the frequency of the applied stimulus.

Other material parameters. The tissue's strength (S_{max}) was defined as the stress' peak value under uniaxial tension. The "uniaxial maximizer strain" [$E(S_{max})$] was taken as the strain at maximum uniaxial stress. The "tangent modulus" (ϵ) was the tangent of the angle between the linear segment of the stress-strain curve, and the work at rupture (ψ) was defined as the area between the stress-strain curve and the strain axis from the origin to the maximizer strain.

All load-displacement curves were converted to stress-strain diagrams by using the relations $S = Fl_o/Al$ (Piola-Kirchoff II) and $E = (l^2 - l_o^2)/2l_o^2$ (Green-Lagrange), with S = stress, F = force, E = strain, and A = PDL cross section. The l_o and l were the resting and strained widths of the PDL, respectively.

Setting the Zero Origin

A typical stress-strain diagram for PDL tissue is shown in Fig. 1. Such curves present a central segment ("zero zone") in which the tissue behaves like a fluid. That is, straining of the sample does not translate into any significant stress response. When moving to the right of this segment (i.e., into the "toe" region), the tissue starts resisting tensile load as the PDL fibers are extended and then continues as a "linear" segment that basically reflects an elastic stretching of the fibers. When further tension is applied to the specimen, the tissue ruptures until final partition. To the left of the zero region, the PDL is compressed between the tooth and the alveolar bone, hence the abrupt increase in compressive stress observed in this segment.

In the zero region no univocal point at which the stress curve transects the *x*-axis may be identified. Therefore the zero origin was defined as follows. First, the strains yielding +5-N (tension) and −5-N (compression) stress responses were determined. Second, the zero origin was set to the intersect of the line connecting the −5- and the +5-N stress levels with the -axis (Fig. 1*A*). This "normative" zero

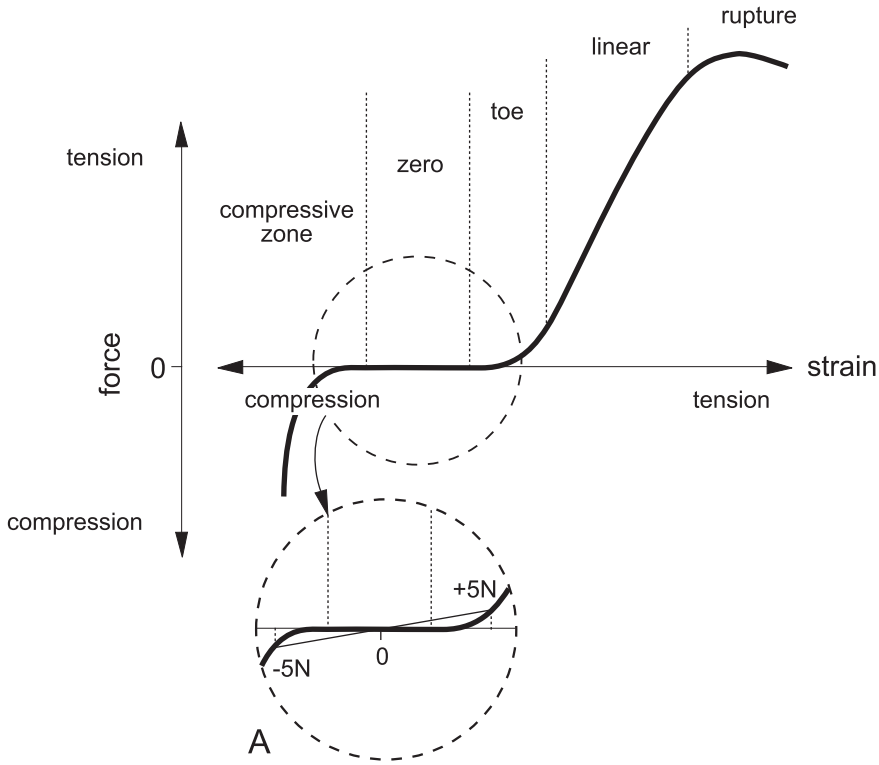

Fig. 1. Typical tension-compression curve for uniaxially strained periodontal ligament (PDL) specimens. Owing to the breadth of the "zero" zone, the location of the zero origin on the *x*-axis is undefined. To define the origin, the specimens were first strained to ±5 N and the corresponding stress levels were registered. The intersect between the connecting line and the *x*-axis was defined as zero (*A*).

was used as the "zero strain" point before and after preconditioning at the onset of the tests.

Specimen Preparation

The test specimens were configured as ~15 × 5 × 2 mm bars that comprised a portion of dentin, PDL, and bone. The specimens were prepared as follows.

Mandibles were obtained from a local abattoir (Vulliamy, Switzerland). To be included into the study, the mandibles had to present fully erupted third molars, thereby indicating an animal age between 3 and 5 yr. Within 3 h of the animal's death, the mandibles were placed in a container refrigerated to 5°C and delivered to the laboratory. At this time bloc sections comprising the first molars were isolated by use of a heavy duty industrial band saw (Magnum, Metabo, Germany), and the soft tissues were removed from the underlying bone. Transverse sections (i.e., near perpendicular to the long axes of the teeth) were obtained by first mounting the blocks into a custom-made chuck that was equipped with a 20-μm resolution dial gauge, thereby ensuring a precise control of the thickness of the sections. Cutting was performed at low feed force (50 g) by using a 0.2-mm-thick, diamond-coated band saw (300 CL/CP, Exakt, Norderstedt, Germany) under abundant saline irrigation. The first cut was placed ~3 mm below the alveolar crest, and this first section was discarded. Then the actual preparing began by placing transverse cuts every 2 mm, resulting in five to six sections. These were labeled as to their depth. After this procedure, the transverse sections were frozen to −21°C in a thermostatized refrigerator (KGE, Bosch, Germany). The entire cutting process lasted about 2 h.

On the day of testing, bar-shaped specimens were cut out of the sections as they thawed by use of the diamond-coated band saw and a custom-made shape guide. As it became available, each specimen was placed in a saline-filled vial and kept at 5°C until testing.

The exact dimensions of the PDL tissue were measured from digital images taken when the specimens were mounted into the testing machine. PDL width and breadth could thus be determined. The thickness of the specimens was measured with a caliper.

The dimensions of a typical bar-shaped specimen are shown in Fig. 2.

Testing Machine

Tensile and compressive tests were conducted using a microtensile machine (Micro Tester 5848, Instron). This device was capable of generating displacement speeds ranging from 3×10^{-4} to 3×10^{3} μm/s with a positional accuracy of 0.5 μm. The machine was set up to apply uniaxial loads to small tissue specimens in a wet environment. A 2-kN load cell (resolution: 0.01 N) was positioned in the axis of measurement. The entire system (actuator displacements and data acquisition) was controlled by a personal computer and the machine's software.

The dentin and bone segment of the specimens were affixed to the machine by custom-made miniature grips. The specimens were fully immersed in saline during testing.

Load Profiles

In a very first series, 15 samples were subjected to ramp tests "as is," that is, shortly after being cut to size and secured to the grips. Each specimen was loaded to a strain of 0.45 at rates of 0.045, 0.44, 0.93, and 1.9 s^{-1} with a rest period of 2 min between each run. Yet the stress responses of the 15 samples tested did not demonstrate any interpretable trend when the strain rate was increased.

It was reasoned that this behavior was attributable to a lack of stability of the tissue structure. Therefore, all subsequent tissue specimens were preconditioned as recommended by Fung (12). That is, they were subjected to 20 tension-compression cycles to a strain amplitude of 0.2 at a frequency of 1 Hz (both these parameters are in line with physiological values). The objective was to load the PDL repeatedly until its internal structure was maintained in a strained state and its rebound to the original (unstrained) condition between two load cycles was minimized (43). At the 20th cycle the stress-strain tracings superimposed (Fig. 3).

In the present experiments four load profiles were applied as shown in Fig. 4. After initial preconditioning, they comprised ramps to 0.5

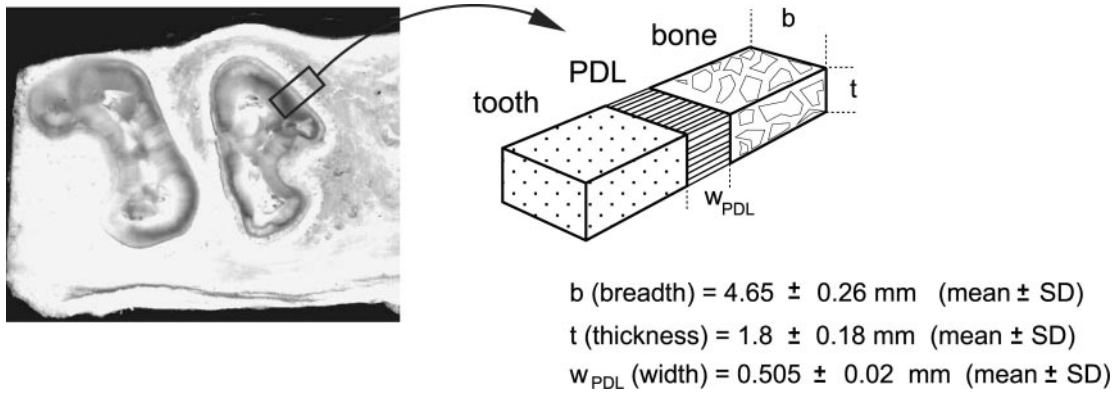

Fig. 2. Specimen production. Bars comprising portions of bone, PDL, and dentin were prepared out of transverse sections of bovine mandibles that comprised molar roots. The overall length of the specimens ranged between 12 and 17 mm.

strain at four different rates, 0.3 and 0.6 discrete and continuous step-strain relaxation, an oscillatory sinusoidal strain between 0.5 and −0.3, and finally a rupture test at three different rates. The specimens were allowed to relax for 2 min between each loading profile. This duration was experimentally determined as the time required for reestablishing a zero load on the load cell. Fifteen valid runs were required for each profile. Although efforts were made to run the specimens through the four profiles consecutively, in many instances either the tissue ruptured unexpectedly or the gripping of the specimens malfunctioned. In these situations, the specimen was discarded and a fresh specimen was preconditioned and the test was started anew.

All specimens from one mandible were pooled, thereby disregarding their original cutting level. Indeed, a parallel study had shown that (with minor exceptions) there was no systematic relation between material parameters and coronoapical location (38).

In excess of 30 mandibles were procured, of which approximately half were used to implement and calibrate the procedure. To obtain 15 valid runs the actual tests were conducted using first molar specimens from 15 mandibles. Whenever a specimen failed before the end of the test, a new specimen from the same mandible was prepared and used. Eventually 67 specimens had been tested.

The tests were planned in terms of tissue strain although they were physically conducted as displacements. This implied a measurement of the specimens' dimensions and a conversion to Lagrangian strains. Hence, before testing, the displacement rate was calculated from the specimen's dimensions.

For the ramp tests, the tissue was strained to 0.5 at rates of $\dot{E}$ = 0.002, 0.04, 0.4, and 1.2 s^{-1}. For the step-strain-relaxation test, the specimens were first strained to 0.3 for 120 s, then allowed to relax and then strained again to 0.6 for 60 s. After another relaxation period, the specimens were strained to 0.3 for 60 s and then to 0.6 for 60 s with no rest in between.

For sinusoidal tests the specimens were subjected to 20 oscillations at frequencies of 0.2 to 5.0 Hz in increments of 0.2 Hz. The strain amplitude was set to −0.3 to +0.5. The phase lag δ, that is, the angular difference between the peak strains and the peak stresses, was determined for the tensile (δ_t) and the compressive (δ_c) components of the cycle (Fig. 5).

Finally, the specimens were divided into three groups and each was pulled to rupture at rates of $\dot{E}$ = 0.002, 0.04, and 1.2 s^{-1}. For the vast majority of specimens, the linear portion of the straining curve was in the 0.4–0.8 range. Besides a further verification of the scaling property, this test also yield the tissue's strength, the peak strain, the maximum tangent modulus, and the strain energy density at rupture.

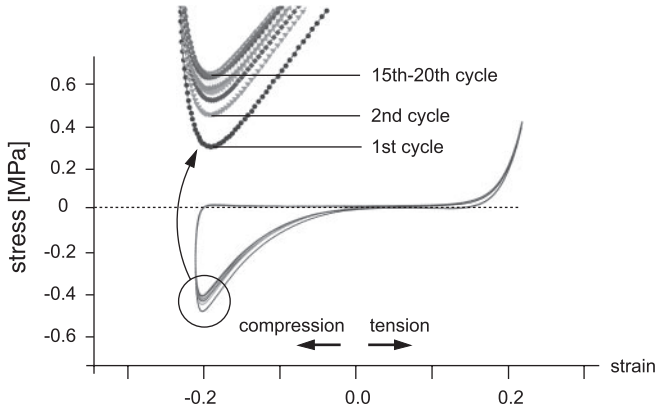

Fig. 3. Tissue preconditioning. After 20 tension-compression cycles at ±0.2 strain, the tracings superimposed and no further rebound was observable.

RESULTS

The experimental data generated during the ramp tests are shown in Fig. 6. After the load-displacement curves were converted to stress-strain diagrams (Fig. 6*A*), stresses and strains were divided by the strain rates for normalization (Fig. 6*B*) (denoted as log$S/\dot{E}$ vs. log$E/\dot{E}$ in the figures). The log-log scale was used due to the large range of the data. As shown, no collapsing occurred. The data rearranged as $S = F(\dot{E})$ for five strain levels are presented in Fig. 7. Therefore, according to the data of Figs. 6 and 7, the PDL's response is not linear. Although the ramps presented in Fig. 6 essentially applied to the physiological range of tooth displacement, Fig. 8 presents the ramps generated during rupture and conducted up to strains of 0.7–0.8 as well as their normalized data. At these strains also the scaling principle was not verified.

The experimental relaxation curves after discrete and continuous step straining are presented in Fig. 9. The computed (i.e., adding both segments of Fig. 9*A*), and experimental two-step curves are shown in Fig. 9*B*. No superposition of the curves was observable; hence the superposition property was not verified.

Figure 10 presents the response to sinusoidal loading at 1, 2, 3, and 4 Hz. The phase lag (plotted as tan δ) between strain and resulting stress for the tensile (δ_t) and compressive (δ_c) half cycle is shown in Fig. 11. The difference between δ_c and δ_t was highly significant ($P < 0.001$). Figure 11 also shows a near stability of the phase lag with respect to frequency.

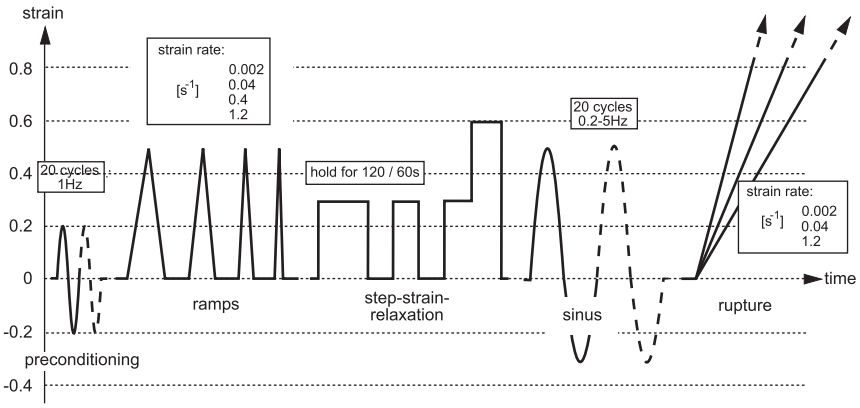

Fig. 4. Load profiles. All samples were first preconditioned and then subjected to *1*) 4 ramps to 0.5 strain at strain rates of 0.002, 0.04, 0.4, and 1.2 s^{-1}; *2*) 2 discrete step-strain relaxation profiles to 0.3 and 0.6 strain followed by a continuous step-strain-relaxation to 0.3 and 0.6; *3*) a sinusoidal strain in the 0.5–0.3 range; and *4*) a rupture test at strain rates of 0.002, 0.04, and 1.2. The specimens were allowed to relax for 2 min between each run.

Besides data for linear scaling assessments (i.e., ramp tests), this test also yield the peak stress (S_{max}), the peak strain [$E(S_{max})$], the maximum tangent modulus (ϵ), and the strain energy density at rupture (ψ) (Table 1).

DISCUSSION

One of the primary objectives of the present study concerned the behavior of the PDL's fluid component. Owing to inherent difficulties in separating experimentally the response of the elastic and viscous components, it was assumed that, at the early deformation phase, the fibers uncoil without supporting significant loads. Thus the fluid dominates the PDL's stress response and $S = \eta\dot{E}$. Under this assumption, the $S = \eta\dot{E}$ relation divided by $\dot{E}$ did not collapse to a straight line, and therefore the viscous contribution was considered not linear. This assertion is also supported by the experimental data on the phase lag shown in Fig. 11. Furthermore, neither the scaling nor the superposition properties were verified for the entire PDL system.

The authors fully realize, however, that the whole postulate must be regarded with caution because it implies that no interaction exists between the κ and the η factors. Hence the relation should be rewritten as $S = \kappa E + \kappa \leftrightarrow \eta$ interaction. The treatment applied herein is an approximation inasmuch as neither the interaction nor the timescale that is necessary to eliminate the effect of κE is known because they depend on the interplay between tissue structure and tissue response.

Modeling the PDL Response

The array of studies in which PDL has been tested under quasi-static conditions justify the conclusion that the PDL's elasticity can be broadly described as "nonlinear stiffening." In contrast, the experiments in which PDL tissue was tested under cyclic loading or in which its creep or stress relaxation re-

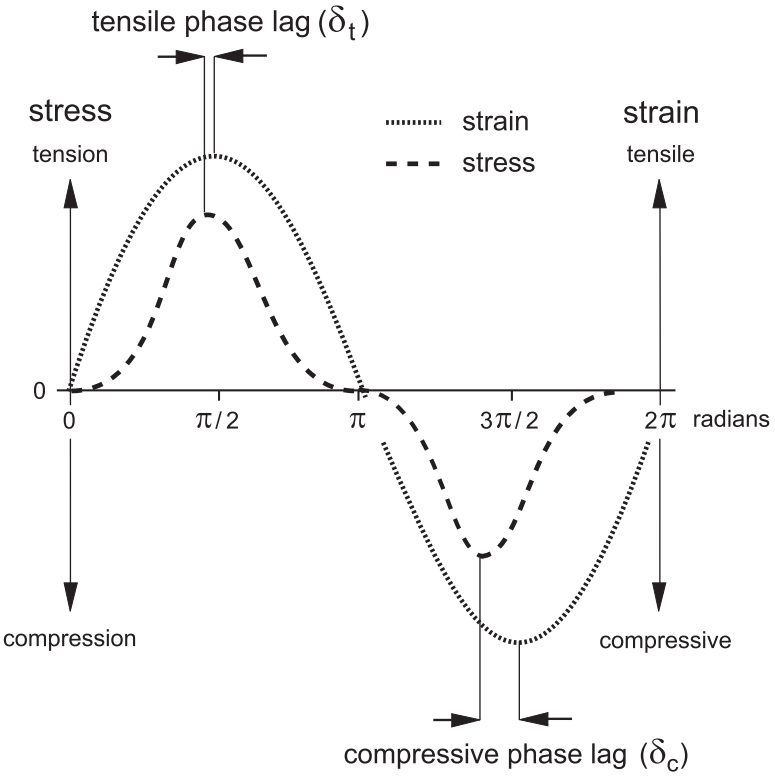

Fig. 5. Phase lag (δ) is the angular difference between peak strains and peak stresses. It may be determined either during the tensile (i.e., δ_t) or during the compressive (i.e., δ_c) components of the load cycle.

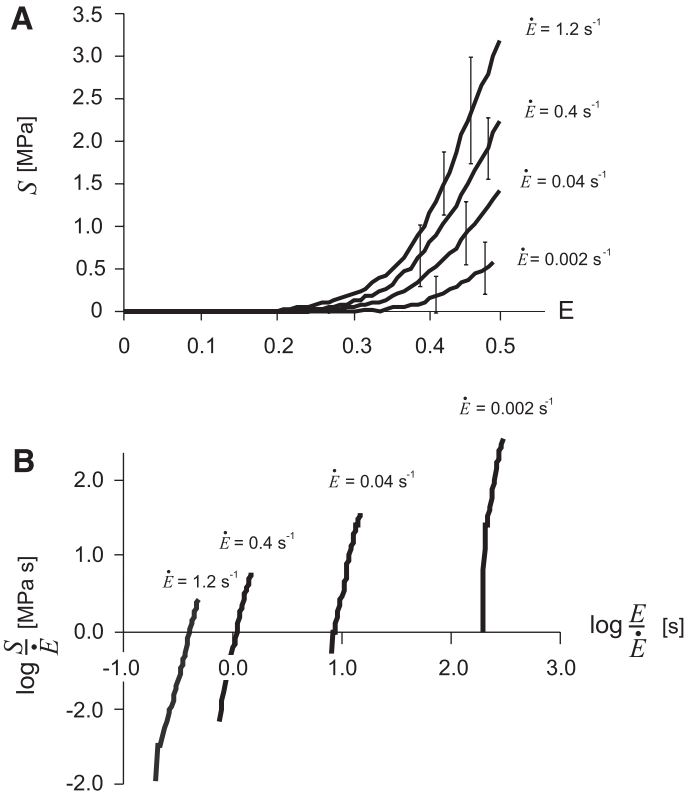

Fig. 6. *A*: stresses recorded for specimens strained to 0.5 at strain rates of 0.002, 0.04, 0.4, and 1.2 s^{-1}. *B*: stresses divided by their respective strain rates for normalization (denoted as $S/\dot{E}$). No collapsing of the curves was observed.

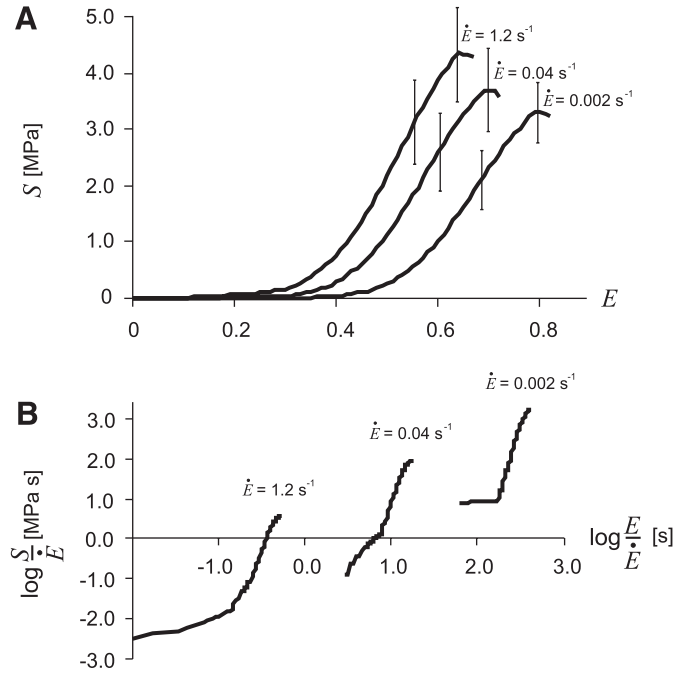

Fig. 8. *A*: stresses recorded for specimens strained to rupture at strain rates of 0.002, 0.04, and 1.2 s^{-1} (vertical bars: SD). *B*: stresses and strains divided by their respective strain rates for normalization (as $S/\dot{E}$). No collapsing of the curves was observed.

sponses were observed gave little insight into its viscoelastic behavior. Bien and Ayers (3) used the Maxwell rheological model (i.e., the spring and the dashpot are mounted in series) to describe the relaxation of a rat tooth, whereas Wills and Picton (29, 46) suggested that a Kelvin-Voigt model (i.e., the spring and dashpot are in parallel) may be used to describe PDL creep. Provatidis (33) used more sophisticated models and finite element techniques to model PDL behavior. Only Middleton et al. (25) have attempted to simulate the PDL's response using a linear viscoelastic law.

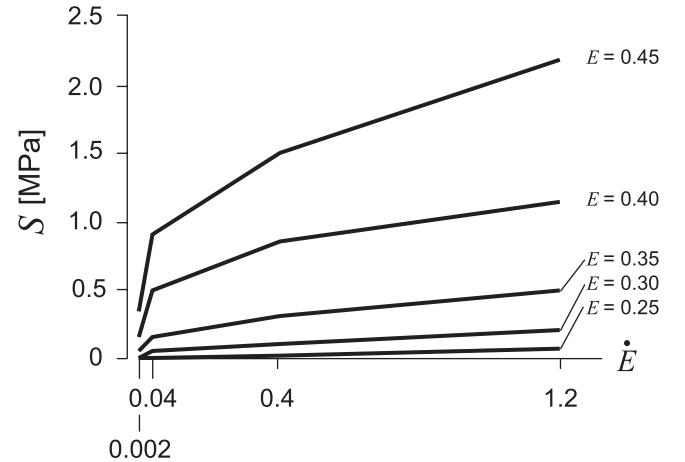

Fig. 7. Stress as a function of the strain rates 0.002, 0.04, 0.4, and 1.2 s^{-1}. Same data set as in Fig. 6.

Attempting to generate nonlinear viscoelastic models would require that large strains and strain rates, nonlinear elasticity, and nonlinear viscosity be included. Stated differently, such a model would consider the geometric kinematic nonlinearities and approach its mechanical behavior as non-Hookean elastic and non-Newtonian viscous. To our knowledge, no models of this complexity have been reported for the PDL.

With respect to our statement in the *Data Analysis* section regarding the need for new analytical techniques for nonlinear viscoelastic systems, the experimental data gathered in the present study led to the development of an equation system that expressed the nonlinearity of both the elastic and the viscous component (19).

In this system the elastic component was expressed as

$$\mathbf{S}(\mathbf{E}) = \kappa|\mathrm{tr}\mathbf{E}|^{c-1}(\mathrm{tr}\mathbf{E})\mathbf{I} + 2\mu\|\mathbf{E}\|^{e-1}\mathbf{E} \quad (\kappa, \mu > 0; c, e > 1)$$

and the viscous component as

$$\mathbf{S}(\dot{\mathbf{E}}) = \kappa'|\mathrm{tr}\dot{E}|^{u-1}(\mathrm{tr}\dot{\mathbf{E}})\mathbf{I} + 2\mu'\|\dot{\mathbf{E}}'\|^{v-1}\dot{\mathbf{E}}' \quad (\kappa',\mu' > 0; 0 < u, v < 1)$$

$\mathbf{S}(\mathbf{E})$ and $\mathbf{S}(\dot{\mathbf{E}})$ are the second-order symmetric elastic and viscous components of stress. $\mathbf{E}$, $\dot{\mathbf{E}}$, and $\dot{\mathbf{E}}'$ are the second-order symmetric strain, strain rate, and strain deviator tensors. $\|\mathbf{E}\|$, tr$\mathbf{E}$, $\|\dot{\mathbf{E}}\|$, and tr$\dot{\mathbf{E}}$ are the norm and trace of $\mathbf{E}$ and $\dot{\mathbf{E}}$, respectively. $\mathbf{I}$ is the second-order unit tensor. In the general three-dimensional load case, each of these tensors has six independent elements characterizing the stress and strain states inside the material. Parameters κ and μ describe (isotropic) bulk and shear elastic properties, and κ' and μ' describe bulk and shear viscous properties. The exponents c, e, u, and v are parameters that characterize the nonlinear behavior of the tissue.

An example of the fitting of these laws to experimental data is shown in Fig. 12. When the equation system was further

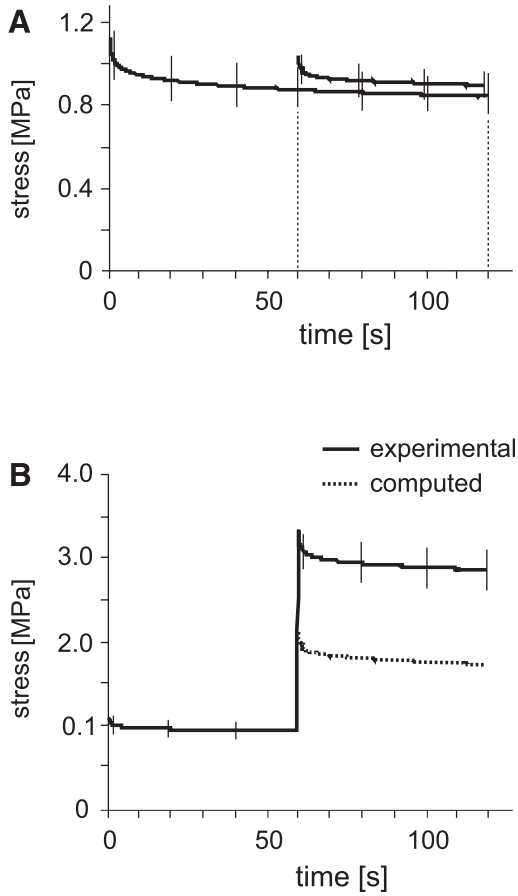

Fig. 9. Experimental relaxation curves after discrete and continuous step-straining (vertical bars: SD). The computed (i.e., adding both segments of *A*) and experimental 2-step curves are shown in *B*. No superposition of the curves was observable.

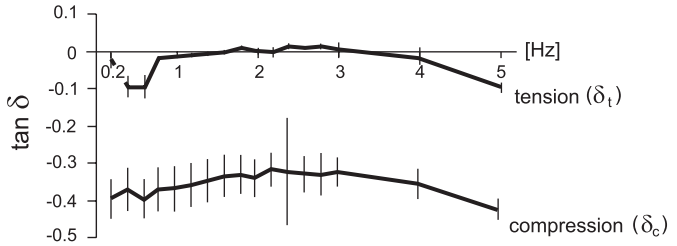

Fig. 11. Phase lag δ (plotted as tan δ) between applied strain and resulting stress for the tensile (δ_t) and compressive half cycle (δ_c) (vertical bars: SD). Note near stability of the phase lag with respect to frequency.

equipped with appropriate elastic (*e*) and viscous (*v*) exponents, it proved adequate to reproduce the stiffening elasticity and thinning viscosity observed with increasing strain rates. Furthermore, the model was able to closely reproduce the nearly flat phase lag-vs.-frequency spectrum graph (Fig. 11), which is a characteristic of biological tissues in general and ligaments in particular (12).

PDL Samples vs. Whole Tooth Experiments

In the past decades, two main avenues were followed to investigate the mechanical response of periodontal ligament. In the first approach, whole teeth of live individuals were subjected to selected load applications, and the resulting movements were recorded (4, 8, 27). The advantage of this approach is that the role of the vasculature is fully accounted for (16, 17). Furthermore, liquid transfer between the PDL tissue and the surrounding alveolar bone during compression or tension occurs under natural conditions. A further refinement consists in generating a finite element mesh of the site under consideration and then duplicating the observed tooth movements by fitting

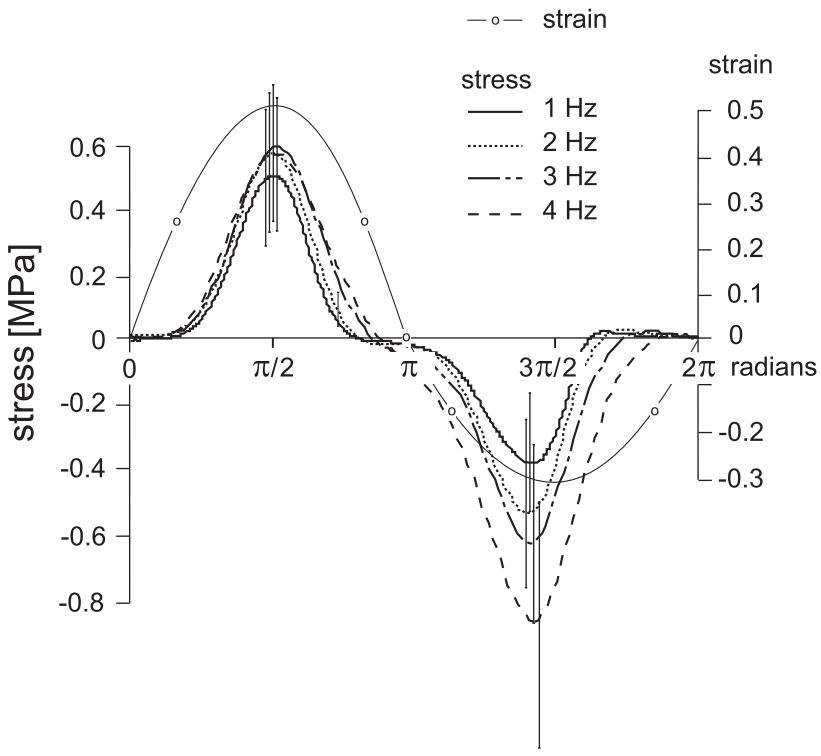

Fig. 10. Stress response to sinusoidal loading at 1, 2, 3, and 4 Hz. Standard deviations are marked at the tensile and compressive peak values. Note alteration in the overall stress response with increasing frequency.

Table 1. *Interaction between strain rate and PDL rupture parameters*

Strain rate	Ė	0.002 s^{-1}	0.04 s^{-1}	1.2 s^{-1}
Tangent modulus, MPa	ε	5.5±2.1	12.5±4.2	19±6.3
Maximizer strain	$E(S_{max})$	0.82±0.19	0.78±0.23	0.61±0.17
Maximum stress, MPa	S_{max}	3.2±0.66	3.7±0.70	4.3±0.75
Strain energy density, MPa	ψ	0.71±0.20	0.73±0.23	0.77±0.25

Values are means ± SD. PDL, peridontal ligament. Means that are not significantly different (Student's *t*-test, 1% level) are connected by horizontal bars.

appropriately parameterized equations into the numerical model (32).

In the present work, the alternate approach was taken in that samples of elementary geometries were used and subjected to mechanical testing with a high degree of control. This approach was deemed necessary because the objective was to formulate constitutive laws (i.e., the equation systems that describe the tissue's behavior) that are based on actual material parameters and not on any best fit function. Stated differently, constitutive laws are "built" by characterizing the material first and then generating equation systems that duplicate experimental data (30). It is this modeling approach that allows the investigator to differentiate between the elastic and the viscous component of the PDL response. The present data confirm the PDL's elastic response as essentially stiffening (concave-convex), which is best represented by a function of the $y = x^3$ type. By contrast, the viscous component is pseudo-plastic or "thinning," which is best described as a cubic root function $y = x^{1/3}$.

By design, in vitro tests on excised specimens will sever the blood supply to the specimens. The effect on the mechanical response, however, should be minor inasmuch as it was shown that loading a tooth to 3.5–5 N obliterates the blood vessels (15) and suppresses the arterial pulsation that may be observed on unloaded teeth (24). Yet normal chewing forces are in the 50- to 100-N range (13). Therefore, it is reasoned that blood pressure essentially stabilizes the teeth at rest and under small loads. This assumption is supported by experimental data on rabbits (28) and a numerical simulation by Walker (45), which indicated that "vasculature does not predominate in tooth support."

To integrate the effects of vasculature and liquid diffusion into the mathematical model, experiments are under way in our laboratory in which samples are encased in a sheath to constrain fluid diffusion and possibly to add pressure while the specimens are loaded.

The sampling and conservation of excised tissue may be a source of variability. In this respect most studies on parallel-fibered ligaments and tendons (44, 48) or on less regularly fibered tissue (36, 40) demonstrated only minor changes in mechanical properties after freezing to −10 to −20°C and subsequent storage. With specific reference to the PDL, Chiba et al. (5) reported that storage in saline for 36 h did not affect the strength of rat PDL. Healing tests have been performed on rat knee ligaments comparing unfrozen with test samples that had been stored in liquid nitrogen at −196°C. With the exception of the strain at failure (−27%), no significant changes were registered in the mechanical properties. It was also found, however, that frozen tissue specimens did not heal as well as unfrozen samples, thereby indicating that freezing interfered with normal tissue biology (21).

The animal's age might also contribute to variability. Indeed, in the present study the cows were aged between 3 and 5 yr at slaughtering. Yet there are indications that age decreases the stiffness of the PDL and reduces the relaxation rate in rats (23). Whether this finding applies to bovines is not known.

Material Properties

As to the actual value of the maximum tangent modulus (in effect the modulus of elasticity), a 1997 report listed 17 publications in which E moduli were used in finite element analyses (34). The values spanned six orders of magnitude ranging from 0.07 to 1,750 MPa. Along with species, location, and strain history, strain rate should also be included in the factors that explain this variation. With varying rates, the PDL fractured at a higher stress level but a lower elongation leading to a fairly constant strain energy density. This indicates the

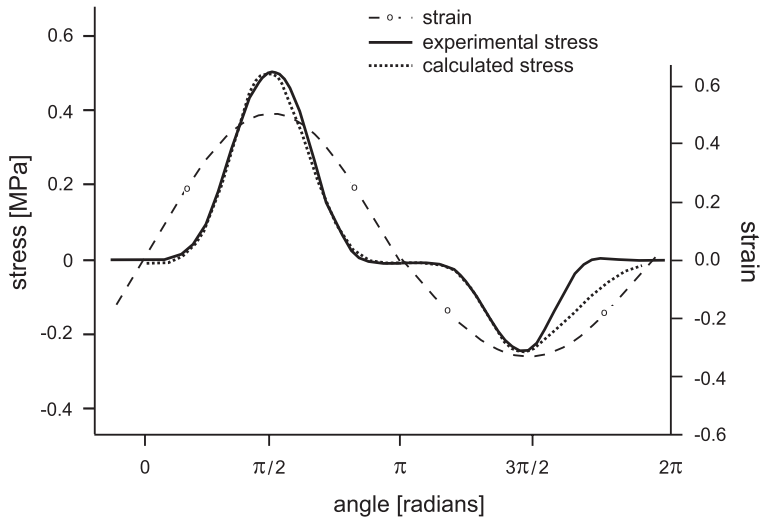

Fig. 12. Example of calculated vs. experimental results. Using the equation system developed from the present experimental data, a calculated curve was fitted onto the data obtained during push-pull cycling of the samples at one Hz.

tissue's capability of incorporating a well-defined amount of energy before rupturing.

Along with the maximizer strain, the maximizer stress, and the maximum tangent modulus, the phase lag (δ) is a material property also. The tangent of δ expresses the ratio between the loss modulus (i.e., the viscous component) and the storage modulus (the elastic component) of the tissue. For PDL in the 0.2- to 5-Hz range, tan δ is small, thereby indicating a dominance of the elastic component. The present data also showed that the phase lags in the compressive and tensile directions were markedly different. This reflects the PDL's anatomical location. Indeed, owing to the multivectorial horizontal force components during chewing (13), PDL is active both in compression (when a portion of the root surface is driven toward the alveolar bone) and in tension (when the same portion is pulled away from the bony housing). In effect the load response of the PDL is essentially controlled by the interplay between the collagen fibers and the surrounding hydrophilic macromolecules and water. The characteristic regular waviness of the fibers is observable in PDL and is referred to as "crimp" (39). Under tensile stress, the fibers first "uncrimp" before starting to stretch and resist displacement. As to the second element (i.e., the ground substance), it consists of 30% glycolipids, glycoproteins, glycosaminoglycans, and proteoglycans and 70% bound water (11). It has been established that most of these macromolecules tend to swell when encased in a collagen matrix. They will also exhibit viscous behavior owing to their resistance to flow under shear loading (26). When placed under compression, this compartment functions like a soft fiber-reinforced composite (18), hence the observed anisotropy in the tensile and compressive directions.

Preconditioning

Whether or not the PDL tissue should have been preconditioned is debatable. Fung (12) recommends preconditioning when presenting mechanical data. Indeed, in the present experiments, preconditioning stabilized the samples and lead to interpretable results. However, in his text, Fung makes his case by stating that tissues are usually stressed in their natural state. Hence after being excised, they would relax and preconditioning would actually revert the tissue to its in vivo (i.e., strained) state. Whether this principle applies to PDL tissue is not known. Undoubtedly, in the present experiment, preconditioning the tissue samples led to results that were in line with expectations. Similar response types might have been generated on unconditioned tissue specimens by a tenfold increase of the number of samples, thereby filtering the "true" response out of the biological variability of the tissue.

Clinical Implications

The ramp tests at increasing strain rates (conducted either to physiological strain or to full rupture) confirm previous reports by Komatsu and Chiba (6, 22). A stiffening at higher loading velocities was expected from a viscoelastic system such as PDL tissue. Such a response has significant clinical implications in particular with respect to the survival of dental bridges that are supported by combinations of natural teeth and osseointegrated implants. Indeed, dental implants are firmly anchored in the alveolar bone (1), whereas the teeth will deflect under lateral pressure (27). Hence the difference in mobility would preclude any mixed (i.e., teeth and implants) support for a solid dental bridge. It has been experimentally demonstrated, however, that under normal chewing conditions (i.e., impact-type loading of the teeth) the viscoelastic stiffening of the PDL was such as to make teeth react similarly to osseointegrated implants (35). Richter's as well as the present data might well explain the favorable outcome of tooth-implant supported restorations (14).

In conclusion, the criteria for linear elastic and linear viscous responses were not met on the PDL of the bovine first molar.

In line with other biological tissues, the PDL's strain-stress phase lag was largely independent of frequency.

ACKNOWLEDGMENTS

Our gratitude is expressed to Dr. A. Mellal and Professor A. Curnier for constructive criticisms and suggestions during the course of this work.

GRANTS

The study was supported by Swiss National Science Foundation Grants 3152-055863.98 and 21-64562.01

REFERENCES

1. **Akin-Nergiz N, Nergiz I, Schulz A, Arpak N, and Niedermeier W.** Reactions of peri-implant tissues to continuous loading of osseointegrated implants. *Am J Orthod Dentofacial Orthop* 114: 292–298, 1998.
2. **Atkinson HF and Ralph WJ.** In vitro strength of the human periodontal ligament. *J Dent Res* 56: 48–52, 1977.
3. **Bien SM and Ayers HD.** Responses of rat maxillary incisors to loads. *J Dent Res* 44: 517–520, 1965.
4. **Brosh T, Machol IH, and Vardimon AD.** Deformation/recovery cycle of the periodontal ligament in human teeth with single or dual contact points. *Arch Oral Biol* 47: 85–92, 2002.
5. **Chiba M, Kinoshita Y, Nakamura G, Ohshima S, Ishikawa S, Tsuruta M, and Ozawa M.** Effects of storage of jaws in saline and of velocity of loading on the force required to extract the rat mandibular first molar. *Arch Oral Biol* 27: 905–907, 1982.
6. **Chiba M and Komatsu K.** Mechanical responses of the periodontal ligament in the transverse section of the rat mandibular incisor at various velocities of loading in vitro. *J Biomech* 26: 561–570, 1993.
7. **Curnier A.** *Computational Methods in Solid Mechanics.* Norwell, MA: Kluwer Academic, 1994.
8. **Daly CH, Nicholls JI, Kydd WL, and Nansen PD.** The response of the human periodontal ligament to torsional loading. I. Experimental methods. *J Biomech* 7: 517–522, 1974.
9. **Decraemer WF, Maes MA, Vanhuyse VJ, and Vanpeperstraete P.** A non-linear viscoelastic constitutive equation for soft biological tissues, based upon a structural model. *J Biomech* 13: 559–564, 1980.
10. **Dorow C, Krstin N, and Sander FG.** Determination of the mechanical properties of the periodontal ligament in a uniaxial tensional experiment. *J Orofac Orthop* 64: 100–107, 2003.
11. **Embery G, Waddington R, and Hall R.** The ground substance of the periodontal ligament. In: *The Periodontal Ligament in Health and Disease*, edited by Berkovitz B, Moxham B, and Newman H. London: Mosby-Wolfe, 1995, p. 83–106.
12. **Fung YC.** *Biomechanics: Mechanical Properties of Living Tissue.* Berlin: Springer, 1993.
13. **Graf H and Geering AH.** Rationale for clinical application of different occlusal philosophies. *Oral Sci Rev* 10: 1–10, 1977.
14. **Gunne J, Astrand P, Lindh T, Borg K, and Olsson M.** Tooth-implant and implant supported fixed partial dentures: a 10-year report. *Int J Prosthodont* 12: 216–221, 1999.
15. **Hofmann M.** Ein weiterer Beitrag zur Frage der Gefässverteilung im Desmodontalraum. *Dtsch zahnärztl Z* 23: 505–508, 1968.
16. **Imamura N, Nakata S, and Nakasima A.** Changes in periodontal pulsation in relation to increasing loads on rat molars and to blood pressure. *Arch Oral Biol* 47: 599–606, 2002.
17. **Ioi H, Nakata S, Nakasima A, Counts AL, and Nanda RS.** Changes in tooth position in humans in relation to arterial blood pressure. *Arch Oral Biol* 47: 219–226, 2002.

18. **Jain MK, Chernomorsky A, Silver FH, and Berg RA.** Material properties of living soft tissue composites. *J Biomed Mater Res* 22: 311–326, 1988.
19. **Justiz J.** *A Nonlinear Large Strain Viscoelastic Law With Application to the Periodontal Ligament* (PhD dissertation). Lausanne: Swiss Federal Institute of Technology, 2004.
20. **Katona TR, Tackney VM, and Keates JK.** A computer model of the periodontal ligament space in man. *Arch Oral Biol* 33: 839–844, 1988.
21. **King GJ, Edwards P, Brant RF, Shrive NG, and Frank CB.** Freezing influences the healing of rabbit medial collateral ligament autografts. *Clin Orthop* 13: 244–253, 1995.
22. **Komatsu K and Chiba M.** The effect of velocity of loading on the biomechanical responses of the periodontal ligament in transverse sections of the rat molar in vitro. *Arch Oral Biol* 38: 369–375, 1993.
23. **Komatsu K, Kanazashi M, Shimada A, Shibata T, Viidik A, and Chiba M.** Effects of age on the stress-strain and stress-relaxation properties of the rat molar periodontal ligament. *Arch Oral Biol* 49: 817–824, 2004.
24. **Korber KH.** Periodontal pulsation. *J Periodontol* 41: 382–390, 1970.
25. **Middleton J, Jones ML, and Wilson AN.** Three-dimensional analysis of orthodontic tooth movement. *J Biomed Eng* 12: 319–327, 1990.
26. **Mow VC, Mak AF, Lai WM, Rosenberg LC, and Tang LH.** Viscoelastic properties of proteoglycan subunits and aggregates in varying solution concentrations. *J Biomech* 17: 325–238, 1984.
27. **Mühlemann HR and Zander HA.** Tooth mobility. III. The mechanism of tooth mobility. *J Periodontol* 25: 128–137, 1954.
28. **Myhre L, Preus HR, and Aars H.** Influences of axial load and blood pressure on the position of the rabbit's incisor tooth. *Acta Odontol Scand* 37: 153–159, 1979.
29. **Picton DC and Wills DJ.** Viscoelastic properties of the periodontal ligament and mucous membrane. *J Prosthet Dent* 40: 263–272, 1978.
30. **Pietrzak G, Curnier A, Botsis J, Scherrer S, Wiskott A, and Belser U.** A nonlinear elastic model of the periodontal ligament and its numerical calibration for the study of tooth mobility. *Comput Methods Biomech Biomed Engin* 5: 91–100, 2002.
31. **Pini M, Wiskott HW, Scherrer SS, Botsis J, and Belser UC.** Mechanical characterization of bovine periodontal ligament. *J Periodontal Res* 37: 237–244, 2002.
32. **Poppe M, Bourauel C, and Jager A.** Determination of the elasticity parameters of the human periodontal ligament and the location of the center of resistance of single-rooted teeth a study of autopsy specimens and their conversion into finite element models. *J Orofac Orthop* 63: 358–370, 2002.
33. **Provatidis CG.** A comparative FEM-study of tooth mobility using isotropic and anisotropic models of the periodontal ligament. Finite Element Method. *Med Eng Phys* 22: 359–370, 2000.
34. **Rees JS and Jacobsen PH.** Elastic modulus of the periodontal ligament. *Biomaterials* 18: 995–999, 1997.
35. **Richter EJ.** In vivo vertical forces on implants. *Int J Oral Maxillofac Implants* 10: 99–108, 1995.
36. **Ridge M and Wright V.** A rheological study of skin. In: *Biomechanics and Related Bio-engineering Topics*, edited by Kennedy R. Oxford, UK: Pergamon, 1965, p. 165–175.
37. **Ross GG, Lear CS, and DeCou R.** Modeling the lateral movement of teeth. *J Biomech* 9: 723–734, 1976.
38. **Shibata T, Botsis J, Bergomi M, Mellal A, and Komatsu K.** Regional effects on the mechanical behavior of bovine's periodontal ligament under tension-compression cyclic displacements. *Eur J Oral Sci*. In Press.
39. **Sloan P and Carter DH.** Structural organisation of the fibres of the periodontal ligament. In: *The Periodontal Ligament in Health and Disease* (2nd ed.), edited by Berkovitz BKB, Moxham BJ, and Newman HN. London: Mosby-Wolfe, 1995, p. 35–53.
40. **Thomas E and Gresham R.** Comparative tensile strength study of fresh, frozen, and freeze-dried human fascia lata. *Surg Forum* 4: 442–443, 1963.
41. **Toms SR, Lemons JE, Bartolucci AA, and Eberhardt AW.** Nonlinear stress-strain behavior of periodontal ligament under orthodontic loading. *Am J Orthod Dentofacial Orthop* 122: 174–179, 2002.
42. **Van Driel WD, van Leeuwen EJ, Von den Hoff JW, Maltha JC, and Kuijpers-Jagtman AM.** Time-dependent mechanical behaviour of the periodontal ligament. *Proc Inst Mech Eng [H]* 214: 497–504, 2000.
43. **Viidik A.** Mechanical properties of parallel-fibered collagenous tissues. In: *Biology of Collagen*, edited by Viidik A and Vuust J. London: Academic, 1980, p. 237–255.
44. **Viidik A, Sandquist L, and Mägi M.** Influence of postmortem storage on tensile strength characteristics and histology of rabbit ligaments. *Acta Orthop Scand* 36, *Suppl* 79: 1–38, 1965.
45. **Walker T.** A model of the periodontal vasculature in tooth support. *J Biomech* 13: 149–157, 1980.
46. **Wills DJ, Picton DC, and Davies WI.** An investigation of the viscoelastic properties of the periodontium in monkeys. *J Periodontal Res* 7: 42–51, 1972.
47. **Wineman A.** Mechanical response of linear viscoelastic solids. *MRS Bull*: 19–23, August 1991.
48. **Woo S, Orlando C, Camp J, and Akeson W.** Effects of postmortem storage by freezing on ligament tensile behavior. *J Biomech* 19: 399–404, 1986.
49. **Yoshida N, Koga Y, Peng CL, Tanaka E, and Kobayashi K.** In vivo measurement of the elastic modulus of the human periodontal ligament. *Med Eng Phys* 23: 567–572, 2001.